The Inositol Polyphosphate 5-Phosphatase Ship Is a Crucial Negative Regulator of B Cell Antigen Receptor Signaling

By Qiurong Liu,* Antonio J. Oliveira-Dos-Santos,* Sanjeev Mariathasan,‡ Denis Bouchard,* Jamie Jones,* Renu Sarao,* Ivona Kozieradzki,* Pamela S. Ohashi,‡§‖ Josef M. Penninger,*‡§ and Daniel J. Dumont*‡

*From the *Amgen Institute, Toronto, Ontario, Canada M5G 2C1; the ‡Department of Medical Biophysics and the §Department of Immunology, University of Toronto, Ontario, Canada M5G 2M9; and the ‖Ontario Cancer Institute, Toronto, Ontario, Canada M5G 2M9*

Summary

Ship is an Src homology 2 domain containing inositol polyphosphate 5-phosphatase which has been implicated as an important signaling molecule in hematopoietic cells. In B cells, Ship becomes associated with Fcγ receptor IIB (FcγRIIB), a low affinity receptor for the Fc portion of immunoglobulin (Ig)G, and is rapidly tyrosine phosphorylated upon B cell antigen receptor (BCR)–FcγRIIB coligation. The function of Ship in lymphocytes was investigated in $Ship^{-/-}$ recombination-activating gene $(Rag)^{-/-}$ chimeric mice generated from gene-targeted $Ship^{-/-}$ embryonic stem cells. $Ship^{-/-}Rag^{-/-}$ chimeras showed reduced numbers of B cells and an overall increase in basal serum Ig. $Ship^{-/-}$ splenic B cells displayed prolonged Ca^{2+} influx, increased proliferation in vitro, and enhanced mitogen-activated protein kinase (MAPK) activation in response to BCR–FcγRIIB coligation. These results demonstrate that Ship plays an essential role in FcγRIIB-mediated inhibition of BCR signaling, and that Ship is a crucial negative regulator of Ca^{2+} flux and MAPK activation.

Key words: inositol phosphatase • Fcγ receptor IIB inhibitory signal • signal transduction • B cell antigen receptor signaling • gene targeting

Ship is an inositol polyphosphate 5-phosphatase that hydrolyzes phosphatidylinositol-3,4,5-polyphosphate (PIP3)[1] and inositol-1,3,4,5-polyphosphate (IP4; references 1 and 2). The catalytic domain of Ship has been shown to reduce the intracellular PIP3 levels and to inhibit the biological effects induced by phosphatidylinositol 3′-kinase activation in *Xenopus* oocytes (3). In addition to the catalytic domain, Ship contains an Src homology (SH)2 domain, three putative SH3 interacting motifs, and two potential phosphotyrosine binding (PTB) domain binding sites. Ship can interact with membrane receptors (4, 5), tyrosine kinases (6), and adapter proteins (7, 8). It has been suggested that Ship functions as a negative regulator of cell growth (2) and as a positive factor in cellular apoptosis (9).

Immune complexes consisting of antigen and IgG antibodies are potent inhibitors of humoral immune responses (10). The immune complex–mediated inhibition of antibody production depends on the coligation of the antigen-specific B cell antigen receptor (BCR) and FcγRIIB, a low affinity receptor for the Fc portion of IgG (11). Engagement of the BCR in the absence of coligation induces rapid activation of tyrosine kinases, generation of inositol phosphates, elevation of the cytoplasmic Ca^{2+} concentration, and mitogen-activated protein kinase (MAPK) activation (12). These events result in cellular activation and lead to B cell proliferation, differentiation, and antibody secretion (13). In contrast, coligation of the BCR and FcγRIIB leads to inhibition of the extracellular Ca^{2+} influx (14), reduction of cell proliferation (15), and blockage of blastogenesis (16).

FcγRIIB delivers the inhibitory signal to downstream SH2-containing proteins through its immunoreceptor ty-

[1]*Abbreviations used in this paper:* BCR, B cell antigen receptor; ERK, extracellular signal–regulated protein kinase; ES, embryonic stem; FBS, fetal bovine serum; Grb, growth factor receptor–bound protein; HSA, heat stable antigen; ICAM, intracellular adhesion molecule; IP4, inositol-1,3,4,5-polyphosphate; ITIM, immunoreceptor tyrosine–based inhibitory motif; JNK, c-Jun NH_2-terminal kinase; MAPK, mitogen-activated protein kinase; PIP3, phosphatidylinositol-3,4,5-polyphosphate; Rag, recombination-activating gene; SAPK, stress-activated protein kinase; SH, Src homology domain; Ship, SH2-containing inositol polyphosphate 5-phosphatase; SHP, SH2-containing protein tyrosine phosphatase; VSV, vesicular stomatitis virus.

rosine–based inhibitory motif (ITIM), a 13–amino acid sequence that is tyrosine phosphorylated in response to BCR and FcγRIIB coligation (17). Several SH2-containing molecules bind to the ITIM of FcγRIIB (18), including the SH2-containing tyrosine phosphatase SHP-1 (19) and the phosphatidylinositol phosphatase Ship (4). SHP-1 was thought to play a significant role in FcγRIIB signaling (15). However, recent studies have shown that SHP-1 is dispensable for FcγRIIB-mediated inhibition of mast cell degranulation (4) and BCR-triggered Ca^{2+} influx (20), suggesting that SHP-1 is not involved in the early signaling events of FcγRIIB inhibition. Another candidate for a key role in FcγRIIB-mediated inhibition is the Ship protein. Ship interacts with the ITIM of FcγRIIB (4) and is rapidly tyrosine phosphorylated in response to BCR–FcγRIIB coligation (21, 22). Deletion of Ship in a chicken B cell line rendered the cells resistant to FcγRIIB-mediated inhibition of Ca^{2+} accumulation (23), suggesting a direct involvement of Ship in the FcγRIIB pathway.

To determine the function of Ship in B and T lymphocytes in vivo, we generated embryonic stem (ES) cell lines with a homozygous mutation in the *Ship* gene and $Ship^{-/-}$ $Rag^{-/-}$ chimeric mice. $Ship^{-/-}Rag^{-/-}$ mice had reduced numbers of B cells, but increased basal serum Igs. $Ship^{-/-}$ B lymphocytes exhibited prolonged Ca^{2+} influx and increased proliferation upon BCR–FcγRIIB coligation, demonstrating an essential requirement for Ship in FcγRIIB-mediated negative signaling. Furthermore, MAPK activation in $Ship^{-/-}$ B cells was increased after BCR–FcγRIIB coligation, suggesting that, once recruited to FcγRIIB, Ship can act as a negative regulator of MAPK signaling.

Materials and Methods

Generation of $Ship^{-/-}Rag\text{-}1^{-/-}$ Mice. A 129/J mouse genomic library was screened with a 300-bp probe which contained the translational initiation codon of the *Ship* gene. Positive clones were characterized by restriction mapping and sequence analysis to determine intron–exon structure and the translation initiation site. A targeting construct was created by first cloning the coding sequences of the *LacZ* gene in-frame with the ATG codon of *Ship*, and then replacing the rest of the *Ship* ATG–containing exon and part of the following intron with a *neo* cassette. A thymidine kinase expression unit was also included for negative selection (24). The linearized targeting vector was electroporated into the 129/Ola-derived ES cell line E14, and colonies were selected in G418 (150 μg/ml; GIBCO BRL, Gaithersburg, MD) and gancyclovir (2 μM/ml; see pp. 33–62 in reference 25). Doubly resistant clones were expanded and DNA samples were digested with HindIII and hybridized to a 3′ external probe to identify recombinants. 4 out of 384 cell lines were heterozygous at the *Ship* locus. DNA from these lines was digested with EcoRV and hybridized to a 5′ HindIII-HindIII internal probe to check for multiple *neo* insertion events. All $Ship^{+/-}$ ES cell lines contained a single *neo* integration. Two independent heterozygous *Ship* clones were cultured at increased concentrations of G418 (1.5 mg/ml) to select for homozygous mutants. Approximately 50% of the surviving clones exhibited homozygous mutation of the *Ship* gene. A parental $Ship^{+/-}$ and three independent $Ship^{-/-}$ ES cell clones were injected into $Rag\text{-}1^{-/-}$ blastocysts. All four ES cell lines contributed to the reconstitution of T and B cell compartments in Rag-1–deficient mice, and all three $Ship^{-/-}Rag^{-/-}$ chimeric mouse strains were similar in phenotype. Mice were maintained at the animal facilities of the Ontario Cancer Institute in accordance with institutional guidelines.

Flow Cytometry. The following FITC-conjugated, PE-conjugated, or biotinylated antibodies were used for flow cytometry: anti-FcγRII/III (clone 2.4G2), anti–TCR-α/β (clone H57-597), anti-CD3ε (clone 145-2C11), anti-CD4 (clone H129.19), anti-CD8α (clone 53-6.7), anti-B220 (clone RA3-6B2), anti-IgD^b (clone 217-170), anti-IgM (clone R6-60.2), anti-CD43 (clone S7), anti-CD19 (clone 1D3), anti-CD25 (clone 7D4), anti-CD24 (anti–heat stable antigen [HSA], clone M1/69), anti-CD40 (clone HM40-3), anti-CD44 (clone 1M7), anti-CD95 (clone Jo2), anti–intracellular adhesion molecule (ICAM)-1 (clone 3E2) (all from PharMingen, San Diego, CA). Biotinylated antibodies were visualized using Streptavidin-Red670 (GIBCO BRL).

Spleen, thymus, lymph node, and bone marrow cells were prepared for flow cytometry according to standard procedures (26). In brief, 2×10^5 cells were incubated at 4°C for 30 min in staining buffer (PBS containing 1% fetal bovine serum [FBS]) with saturating amounts of antibodies against lineage-specific surface antigens. Cells were washed with staining buffer and incubated with streptavidin-Red670 at 4°C for another 30 min. After washing with staining buffer, cells were analyzed using a FACSCalibur® flow cytometer and CELLQuest software (Becton Dickinson, Mountain View, CA).

In Vitro B Cell Proliferation. Splenic lymphocytes from 8–14-wk-old mice were incubated in 0.155 M ammonium chloride, 0.1 mM sodium EDTA, 0.1% potassium bicarbonate, pH 7.3, for 5 min on ice to lyse red blood cells. Cells were washed with PBS and incubated with anti–Thy-1, anti-CD8, and anti-CD4 in combination with rabbit complement (Cedarlane Labs Ltd., Hornby, Ontario, Canada) for complement-mediated lysis of T cells. Lymphocytes were collected from the interface of a lympholyte purification gradient (Lympholyte-M; Cedarlane Labs Ltd.). The purity of each of the splenic B cell preparations was verified by flow cytometric analysis, and was typically ≥85%.

Purified splenic B cells (5×10^4/100 μl) were cultured in triplicate in RPMI medium supplemented with 5% FBS, 2 μM sodium pyruvate, 1 μM glutamine, 50 μM β-mercaptoethanol, and antibiotics at 37°C for 3 h. Goat anti–mouse IgM (Jackson ImmunoResearch Laboratories, West Grove, PA), the $F(ab')_2$ fragment of goat anti–mouse IgM (Jackson ImmunoResearch Laboratories), LPS (Sigma Chemical Co., St. Louis, MO), or anti-CD40 antibody was added to the culture medium at various concentrations. Cells were incubated in triplicate for 48–72 h followed by the addition of 1 μCi/well [^{3}H]thymidine (Nycomed Amersham plc, Little Chalfont, Bucks, UK). Cells were harvested 6 h after thymidine addition, and the amount of [^{3}H]thymidine incorporation was determined using a β-scintillation counter (Coulter Corp., Miami, FL).

In Vitro T Cell Proliferation. Freshly isolated lymphocytes from lymph nodes were placed into round-bottomed 96-well plates (Fisher Scientific, Nepean, Ontario, Canada) in RPMI medium supplemented with 5% FBS, 2 μM sodium pyruvate, 1 μM glutamine, 50 μM β-mercaptoethanol, and antibiotics. Cells were activated with PMA (10 μg/ml) plus Ca^{2+} ionophore A23617 (100 ng/ml), soluble anti-CD3ε (0.2 μg/ml, clone 145-2C11, hamster IgG; PharMingen), and soluble anti-CD28 (0.02 μg/ml and 0.2 μg/ml, clone 37.51, hamster IgG; PharMingen) in triplicate for 48 h followed by the addition of [^{3}H]thymidine and analysis as described above.

Intracellular Ca^{2+} Measurements. Splenocytes (5×10^6/ml) were loaded with 3 μM Indo-1 (Molecular Probes, Inc., Eugene, OR) at 37°C for 1 h in IMDM supplemented with 2% FCS. After washing with medium, cells were labeled with PE-conjugated anti–TCR-α/β antibody to remove T cells by gating. B cells were stimulated by the addition of intact rabbit anti–mouse IgG (Zymed Laboratories, Inc., South San Francisco, CA) or the $F(ab')_2$ fragment of rabbit anti–mouse IgG (Zymed Laboratories, Inc.). Cells were stimulated with a titration series of each antibody to determine optimal conditions. Cytosolic Ca^{2+} flux of 10^6 cells was recorded using a FACSVantage® (Becton Dickinson). Ca^{2+} mobilization from intracellular stores was measured in the presence of 2 mM EGTA. Thymocytes (5×10^6/ml) were loaded with 5 μM Indo-1 following the same procedure except that cells were incubated with 5 μg/ml anti-CD3ε or 5 μg/ml anti-CD3ε plus 1 μg/ml anti-CD28 in ice for 15 min, and Ca^{2+} flux was recorded immediately after the addition of 30 μg/ml anti–hamster IgG.

Western Blot Analysis. Purified splenic B cells (2×10^6 cells/100 μl PBS) were stimulated with PBS alone, goat anti–mouse IgM antibody (20 μg/ml), the $F(ab')_2$ fragment of goat anti–mouse IgM (15 μg/ml), LPS (2 μg/ml), or anti-CD40 antibody (5 μg/ml) at 37°C for various time periods. At the end of the stimulation, cells were immediately diluted with 1 ml ice-cold PBS containing 1 mM sodium vanadate (Na_3VO_4), pelleted by centrifugation, and resuspended in 20 μl ice-cold lysis buffer consisting of 1% Triton X-100, 1% deoxycholate, 50 mM Hepes buffer, pH 7.4, 150 mM NaCl, 10% glycerol, 1.5 mM $MgCl_2$, 1 mM EGTA, 100 mM NaF, 1 mM PMSF, and 1 mM Na_3VO_4. Cell debris was pelleted, and supernatants containing the whole cell lysates were analyzed on 15% SDS–polyacrylamide gels at an acrylamide to bis-acrylamide ratio of 120:1. Proteins were transferred to nitrocellulose membranes and immunoblotted with phospho-specific P44/P42 MAPK antibody (Thr202/Tyr204; New England Biolabs Inc., Beverly, MA) to reveal the presence of activated MAPK; phospho-specific stress-activated protein kinase (SAPK)/c-Jun NH_2-terminal kinase (JNK) antibody (New England Biolabs Inc.) to reveal the presence of activated SAPK/JNK; and phospho-specific IκB antibody (New England Biolabs Inc.) to reveal nuclear factor κB activation. To verify equivalent loading and to confirm the identity of the phosphorylated MAPK, membranes were stripped with 100 mM β-mercaptoethanol, 2% SDS, 62.5 mM Tris (pH 6.7) at 55°C for 30 min and blotted with anti–extracellular signal–regulated protein kinase (ERK)2 antibody (Transduction Laboratories, Lexington, KY). Immunoblots were visualized with enhanced chemiluminescence detection reagents (ECL; Nycomed Amersham plc).

Freshly isolated thymocytes were incubated with 10 μg/ml of rabbit anti–hamster IgG on ice for 15 min followed by stimulation with anti-CD3ε or anti-CD3ε plus anti-CD28 at 37°C for various time periods (1–15 min). Activation was stopped by the addition of ice-cold PBS containing 1 mM Na_3VO_4. Cells were lysed and analyzed as described above.

Detection of Ig Levels. ELISA for Ig subclasses was performed on serially diluted serum samples using anti–mouse Ig (IgG plus IgA plus IgM) antibodies and alkaline phosphatase–conjugated anti–mouse Ig isotype antibodies (Southern Biotechnology Associates, Inc., Birmingham, AL) according to the manufacturer's directions.

Serum Neutralization Test. Vesicular stomatitis virus (VSV) Indiana (Mudd-Summers isolate) seeds were grown on BHK21 cells infected with a low multiplicity of infection and plaqued on Vero cells. Sera were collected from mice at defined time points after VSV infection. The sera were prediluted 40-fold in MEM containing 5% FCS and then heat-inactivated at 56°C for 30 min. Serial twofold dilutions were mixed with equal volume of VSV-containing medium (500 PFU/ml) and incubated in a 5% CO_2 incubator at 37°C for 90 min. 100 μl of the mixture was transferred onto Vero cell monolayers in 96-well plates and incubated at 37°C for 1 h. The monolayers were then overlaid with 100 μl of DMEM containing 1% methylcellulose. After incubating at 37°C for 24 h, the monolayer was fixed and stained with 0.5% crystal violet. The highest dilution of serum that reduced the number of plaques by 50% was taken as titer. To determine IgG titers, undiluted serum was pretreated with an equal volume of 0.1 mM β-mercaptoethanol in saline to eliminate IgM.

In Vitro Th Cell Differentiation. Splenocytes (2×10^6/ml) depleted of red blood cells were cultured in duplicate in RPMI medium supplemented with 5% FBS, 50 μM β-mercaptoethanol, and 1× penicillin-streptomycin (GIBCO BRL), and were stimulated with 10 μg/ml plate-bound anti-CD3ε in the presence of 1 ng/ml IL-12 (PharMingen) for Th1 or 50 ng/ml IL-4 (PharMingen) for Th2 differentiation. After 5 d incubation, cells were washed in PBS, and an equal number of viable cells was replated in 10 μg/ml plate-bound anti-CD3ε in the absence of cytokine addition. Supernatants were collected 24 h later, and the production of IFN-γ and TNF-α from Th1-differentiated or of IL-4 and IL-6 from Th2-differentiated cultures was measured in duplicate by ELISA assay (Genzyme Corp., Cambridge, MA).

Results

Generation of $Ship^{-/-}Rag^{-/-}$ Chimeric Mice. Targeted inactivation of the *Ship* gene in ES cells was accomplished by replacement of the first coding exon and part of the following intron with the *LacZ* gene from *Escherichia coli* and the gene encoding neomycin phosphotransferase (*neo*) (Fig. 1 *A*). $Ship^{-/-}$ ES cells were isolated by selecting $Ship^{+/-}$ ES cells in elevated levels of G418. Homozygous mutation of the *Ship* gene was confirmed by Southern blot analysis of genomic DNA (Fig. 1 *B*). Three different $Ship^{-/-}$ clones and a parental $Ship^{+/-}$ ES cell clone were injected into blastocysts from $Rag\text{-}1^{-/-}$ mice. Since Rag-deficient mice do not produce any mature lymphocytes due to a block in the initiation of V(D)J recombination (27), mature lymphocytes in the chimeric mice must be derived from the injected ES cells. Chimeric mice were characterized by flow cytometric analysis of $CD4^+$ and $CD8^+$ T cells and IgD^+ B cells in circulating blood. Genetic chimerism was further substantiated by Southern blot analysis of DNA obtained from tail biopsies (data not shown). Western blot analysis of lysates prepared from thymocytes (data not shown) and splenocytes (Fig. 1 *C*) of the $Ship^{-/-}Rag^{-/-}$ chimeras showed the absence of Ship protein, indicating that the engineered *Ship* mutation was a null mutation. All chimeric mice appeared healthy and had no apparent abnormalities.

Increased Numbers of Peripheral T cells, but Normal T Cell Proliferation in $Ship^{-/-}Rag^{-/-}$ Mice. The thymus and lymph nodes were of normal size in $Ship^{-/-}Rag^{-/-}$ chimeric mice, but the spleen was significantly enlarged. The total number of thymocytes and the percentages of $CD4^-CD8^-$

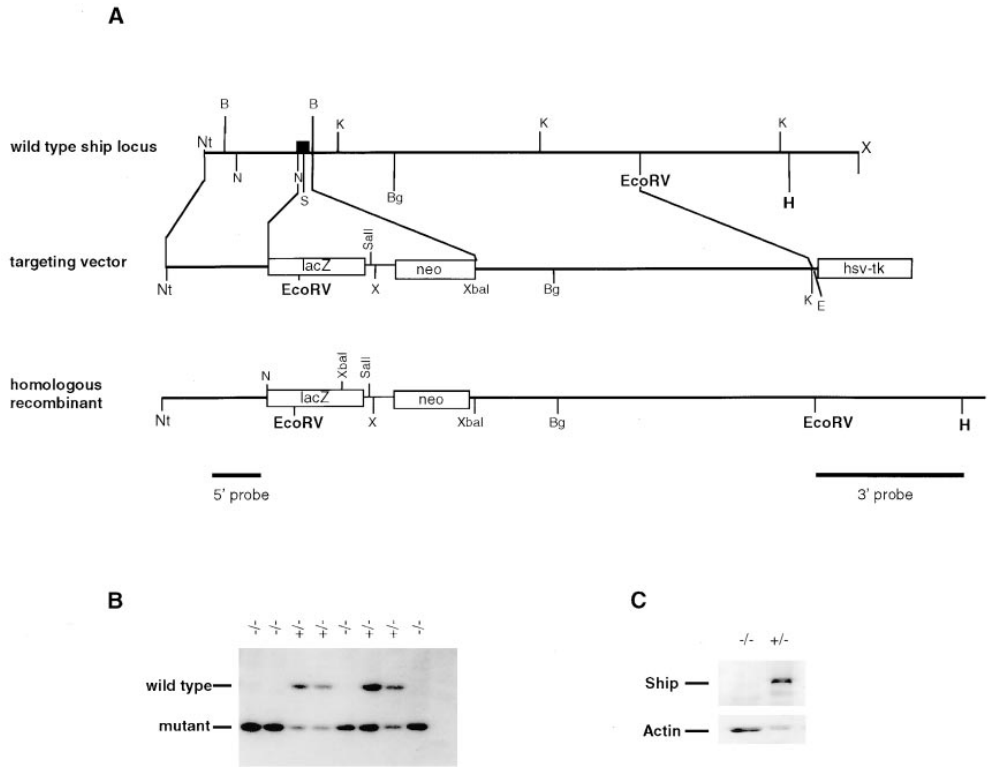

Figure 1. Gene targeting of the *Ship* locus. (*A*) Targeting vector. A 1-kb NcoI-BamHI fragment was replaced by the *LacZ* gene and the neomycin resistance (*neo*) gene. The coding sequence of the *LacZ* gene was cloned in-frame with the *Ship* ATG codon by using the NcoI site immediately downstream of the ATG codon. The HSV-*tk* gene was appended to allow for selection against random integration. 1.8 and 5 kb of homologous sequences flanking the replacement were retained. The predicted structure of the disrupted allele is shown. *Black box*, The exon. *Nt*, Not1; *B*, BamHI; *N*, NcoI; *S*, SmaI; *K*, KpnI; *Bg*, BglII; *H*, HindIII; *X*, XhoI; *E*, EcoRI. (*B*) Southern blot showing homozygous Ship$^{-/-}$ ES cell lines created through selection of Ship$^{+/-}$ lines in a high concentration of G418. Genomic DNA from ES cells was digested with EcoRV and hybridized to a 5′ internal probe to visualize a 10.5-kb band for the wild-type allele and a 5.8-kb band for the mutant allele. (*C*) Western blot analysis of Ship$^{-/-}$ lymphocyte proteins. Protein extracts from 2×10^6 purified splenic B cells of Ship$^{+/-}$Rag$^{-/-}$ and Ship$^{-/-}$Rag$^{-/-}$ mice were hybridized to anti-Ship antibody raised against amino acid residues 276–450 (reference 47). The position of Ship is indicated. The nitrocellulose membrane was then stripped and rehybridized to anti-actin antibody to control for the amount of protein loaded in each lane.

pre-T cells and CD4$^+$CD8$^+$ immature T cells in Ship$^{-/-}$Rag$^{-/-}$ mice were similar to those found in Ship$^{+/-}$Rag$^{-/-}$ mice (Table 1), showing that early thymic development was normal. However, the ratio of mature CD4$^+$ to CD8$^+$ T cells was higher in Ship$^{-/-}$Rag$^{-/-}$ compared with Ship$^{+/-}$Rag$^{-/-}$ chimeric mice, suggesting an effect of the mutation on the progression of immature CD4$^+$CD8$^+$ thymocytes to mature CD4$^+$ and CD8$^+$ T cells and/or CD4/CD8 homeostasis in peripheral lymphoid organs (Table 1). No abnormalities were found in the surface expression levels of TCR-α/β, CD3, CD28, or CD95 on either CD4$^+$ or CD8$^+$ single positive thymocytes, CD4$^+$CD8$^+$ double positive thymocytes, or peripheral T cells (data not shown).

To test the role of Ship in T cell proliferation, lymph node T cells were stimulated in vitro with either anti-CD3ϵ antibody, anti-CD3ϵ plus anti-CD28 antibodies, Con A, or PMA plus Ca^{2+} ionophore. No significant differences in the extent or kinetics of proliferation or IL-2 production were observed between the Ship$^{+/-}$ and Ship$^{-/-}$ T cells (data not shown). Similarly, no obvious differences were observed in the levels of phosphorylated IκB, MAPK, or SAPK between Ship$^{+/-}$ and Ship$^{-/-}$ T cells after anti-CD3ϵ or anti-CD3ϵ plus anti-CD28 stimulation (data not shown). The extent and duration of Ca^{2+} mobilization also appeared to be normal in Ship$^{-/-}$ thymocytes activated with anti-CD3ϵ or anti-CD3ϵ plus anti-CD28 (data not shown).

Reduced Numbers of B Cells in Ship$^{-/-}$Rag$^{-/-}$ Mice. To examine the effect of the Ship mutation on B cell development, single cell suspensions from spleen and bone marrow of Ship$^{+/-}$Rag$^{-/-}$ and Ship$^{-/-}$Rag$^{-/-}$ chimeras were stained with mAbs against B lineage–specific markers. The bone marrow of Ship$^{-/-}$Rag$^{-/-}$ chimeric mice had normal numbers of B220$^+$CD43$^+$ pro-B cells but significantly reduced numbers of B220$^+$sIgM$^+$ immature and B220$^+$sIgD$^+$ mature B cells (Fig. 2, and Table 1), suggesting a partial maturational defect of Ship$^{-/-}$ B cells. We found that B cell numbers were also reduced in the B220$^+$sIgM$^-$ population that expresses the IL-2Rα chain (CD25; Table 1), an early B cell maturation marker that appears in the small pre-B stage before sIgM expression (28). Consistent with this finding, Ship$^{-/-}$Rag$^{-/-}$ mice showed normal percentages of B220^{lo}HSA^{hi} large pre-B cells, but significantly reduced percentages of the more mature B220$^+$HSA^{lo} population (Table 1). These results suggest that B cell production is normal in Ship$^{-/-}$Rag$^{-/-}$ chimeric mice until the B220$^+$CD43$^+$ large pre-B stage, but fewer B cells were present in the small pre-B and more mature populations.

Peripheral B cells from Ship$^{-/-}$Rag$^{-/-}$ chimeras expressed normal cell surface levels of CD19, CD40, CD44, ICAM-1, and CD95, but reduced levels of CD23 (data not shown). Closer examination of splenic B cell subpopulations revealed a decrease in the sIgM^{hi}sIgD^{hi} population with a shift towards the more mature sIgM^{lo}sIgD^{hi} pheno-

Table 1. *T and B Cell Subpopulations in Ship$^{-/-}$Rag$^{-/-}$ Chimeric Mice*

	Ship$^{+/-}$Rag$^{-/-}$	Ship$^{-/-}$Rag$^{-/-}$
Thymus		
Total cell number ($\times 10^7$)	8 ± 0.6	8.6 ± 0.9
CD4$^+$CD8$^+$ (% ± SEM)	81.5 ± 4.1	76.6 ± 4.9
CD4$^+$CD8$^-$	13.3 ± 3.2	17.6 ± 3.9
CD4$^-$CD8$^+$	2.3 ± 1.0	2.8 ± 0.8
CD4$^-$CD8$^-$	2.9± 0.2	3.1 ± 0.4
Lymph nodes		
Total cell number ($\times 10^7$)	2.4 ± 0.6	2 ± 0.5
CD4$^+$CD8$^-$ (% ± SEM)	58.3 ± 3.1	**68.5 ± 3.5**
CD4$^-$CD8$^+$	17.8 ± 2.8	13.4 ± 2.5
Spleen		
Total cell number ($\times 10^7$)	6.5 ± 0.4	11 ± 1.2
CD4$^+$CD8$^-$ (% ± SEM)	29.2 ± 4.9	**47.4 ± 3.1**
CD4$^-$CD8$^+$	13.8 ± 2.0	9.4 ± 4.8
B220$^+$sIgM$^+$	36 ± 5.5	**27 ± 4.5**
sIgD$^+$sIgM^{hi}	10.7 ± 2.0	**4.7 ± 1.7**
sIgD^{hi}sIgM^{lo}	24.2 ± 4.1	**20 ± 3.5**
Bone marrow		
Total cell number ($\times 10^7$)	1.2 ± 0.3	1.4 ± 0.3
B220$^+$CD43$^+$ (% ± SEM)	8.5 ± 3.3	9.8 ± 2.4
BD220$^+$CD43$^-$	45.4 ± 4.6	**19.1 ± 2.9**
B220$^+$CD25$^+$IgM$^-$	7.1 ± 1.4	**4.5 ± 1.0**
B220^{lo}HSA^{hi}	26.4 ± 4.2	25.3 ± 2.6
B220$^+$HSA^{lo}	16 ± 3.1	**4.9 ± 1.2**
B220$^+$sIgM$^+$	16.4 ± 2.1	**8.7 ± 2.5**

Cells from Ship$^{+/-}$ (n = 5) and Ship$^{-/-}$ (n = 7) chimeric mice were stained with the indicated antibodies, and populations were determined using a FACScan®. **Bold numbers**, Statistically significant differences between Ship$^{+/-}$ and Ship$^{-/-}$ subpopulations.

type (Fig. 2). This shift is probably not a consequence of lowered sIgM expression due to the *Ship* mutation, since the level of sIgM expression is normal in Ship$^{-/-}$ B cells in the bone marrow (Fig. 2). We favor the hypothesis that this shift reflects an augmented maturational event occurring in Ship$^{-/-}$ B lymphocytes.

Higher Titers of Serum Ig and Normal Anti-VSV Response of Ship$^{-/-}$Rag$^{-/-}$ Mice. To assess the functional consequences of Ship deficiency, we analyzed the production of Igs in Ship$^{-/-}$Rag$^{-/-}$ chimeric mice. Sera from unimmunized Ship$^{-/-}$Rag$^{-/-}$ chimeras showed an overall increase in Ig levels despite a reduction in the number of peripheral B cells. In particular, IgM, IgA, IgG2a, and IgG2b levels were elevated, whereas IgG1 levels were reduced (Fig. 3 *A*).

To further characterize the functional significance of the Ship deficiency in vivo, chimeric mice were immunized with VSV. Unexpectedly, antivirus-specific antibody production occurred at a normal level and with similar kinetics in the T help–independent neutralizing IgM response as well as in T cell–dependent class switching from IgM to IgG (29; Fig. 3 *B*). Moreover, similar titers of neutralizing IgG were detected for both Ship$^{+/-}$Rag$^{-/-}$ and Ship$^{-/-}$Rag$^{-/-}$ mice 80 d after immunization (Fig. 3 *B*, and data not shown), although the levels of nonneutralizing Ig were significantly higher in Ship$^{-/-}$Rag$^{-/-}$ chimeras (data not shown). These results show that Ship is not essential to maintain the homeostasis of VSV-neutralizing IgM and IgG responses, and suggest that multiple negative signaling molecules regulate in vivo B cell responses.

Normal Production of Th1 and Th2 Cytokines by Ship$^{-/-}$ T Cells. The reduced level of serum IgG1, an IL-4–driven Ig isotype, and the increased level of IgG2a, which depends on IFN-γ for Ig class switching, suggested that Th cell differentiation might be affected in Ship$^{-/-}$ T cells. Therefore, we examined the response of Ship$^{-/-}$ T cells to two different stimuli known to induce the differentiation of Th1 and Th2 cells. Ship$^{-/-}$ splenocytes stimulated with anti-CD3ε in the presence of IL-4, which induces Th2 differentiation, showed normal levels of IL-4 and IL-6 production. Similarly, when Ship$^{-/-}$ T cells were stimulated with anti-CD3ε in the presence of IL-12, which induces Th1 differentiation, there was no significant difference between Ship$^{-/-}$ and Ship$^{+/-}$ cells in the production of Th1-type cytokines IFN-γ and TNF-α (data not shown). Although these results do not preclude a role of Ship in Th1 and Th2 cytokine production in vivo, our in vitro data imply that Ship has no essential role in Th1 and Th2 lineage differentiation.

Increased Proliferation of Ship$^{-/-}$ B Cells upon BCR–FcγRIIB Coligation. To test the hypothesis that Ship downregulates B cell activation (23), B cell proliferation in Ship$^{-/-}$Rag$^{-/-}$ chimeric mice was examined. BCR signaling can be activated by the F(ab′)$_2$ fragment of anti-IgM (or anti-IgG) antibodies that cause cross-linking of sIgM (or sIgG; reference 11). Intact antibodies fail to stimulate BCR-mediated cellular activation because they coligate the BCR and FcγRIIB (11), resulting in activation of the FcγRIIB inhibitory pathway. When sIgM was cross-linked on purified Ship$^{-/-}$ and Ship$^{+/-}$ B cells using the F(ab′)$_2$ fragment of anti-IgM, comparable proliferative responses were induced, suggesting that BCR signaling is normal in Ship$^{-/-}$ B cells (Fig. 4). However, whereas coligation of sIgM and FcγRIIB with intact anti-IgM did not significantly stimulate proliferation in Ship$^{+/-}$ cells, Ship$^{-/-}$ B cells proliferated just as strongly in response to intact antibody as they had in response to anti-IgM F(ab′)$_2$ stimulation (Fig. 4). Similar, but less dramatic, results were obtained using anti–mouse IgG (data not shown). No differences in proliferation were detected when Ship$^{-/-}$ and Ship$^{+/-}$ B cells were stimulated with LPS or anti-CD40, agents that do not use the FcγRIIB pathway (30, 31; Fig. 4 *B*). These results show that Ship is required for the delivery of a negative regulatory signal in response to BCR–FcγRIIB coligation.

Prolonged Ca^{2+} Mobilization in Ship$^{-/-}$ B Cells upon BCR–FcγRIIB Coligation. A well-documented effect of BCR and FcγRIIB coligation is the inhibition of extracel-

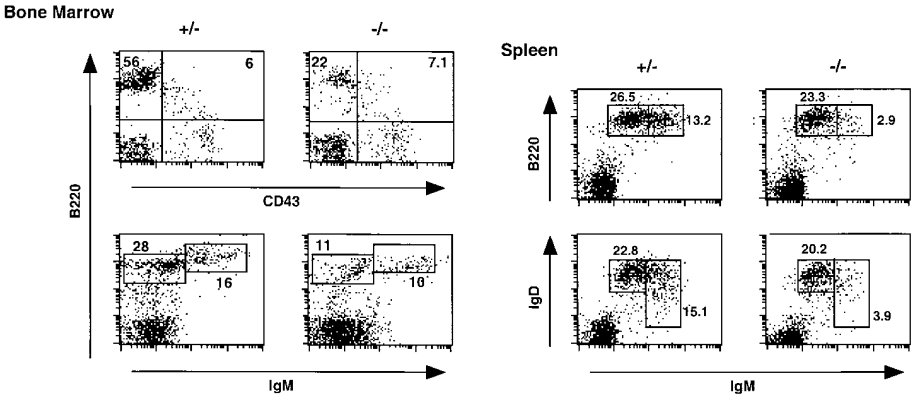

Figure 2. Flow cytometric analysis of lymphocytes from Ship$^{-/-}$Rag$^{-/-}$ chimeric mice. Total lymphocytes from bone marrow and spleen were stained with lineage-specific antibodies as indicated. *Boxes*, Percentages of distinct subpopulations of B cells. One result representative of five different experiments is shown.

lular Ca^{2+} influx (14, 20, 23). To determine whether Ship acts by downregulating the Ca^{2+} influx associated with BCR stimulation, we compared Ca^{2+} mobilization in Ship$^{+/-}$ and Ship$^{-/-}$ B lymphocytes after sIg activation or sIg–FcγRIIB coligation. Ship$^{+/-}$ B cells activated with the $F(ab')_2$ fragment of anti-IgG exhibited a rapid increase in intracellular free Ca^{2+} (Fig. 5 *B*), a response that was reduced in Ship$^{+/-}$ B cells stimulated with intact anti-IgG antibody. In contrast, an increased and prolonged Ca^{2+} response was observed in Ship$^{-/-}$ B cells stimulated with intact anti-IgG antibody (Fig. 5 *B*), despite normal FcγRIIB expression on the cell surface (Fig. 5 *A*). This increased Ca^{2+} response to intact anti-IgG could be normalized to the level observed in Ship$^{+/-}$ B cells by the addition of the Ca^{2+} chelator EGTA, which exhausts the extracellular Ca^{2+} store (data not shown). These data suggest that Ship acts as negative regulator in the FcγRIIB pathway by controlling the Ca^{2+} influx.

Enhanced ERK2 Phosphorylation in Ship$^{-/-}$ B Cells upon BCR–FcγRIIB Coligation. BCR signaling has also been shown to activate the ERK2 isoform of MAPKs (32, 33). This activation is accompanied by an increase in phosphorylation of ERK2 (34). To test whether Ship is involved in the MAPK pathway, we examined ERK2 phosphorylation after BCR activation. As shown in Fig. 6, ERK2 was activated equally in Ship$^{+/-}$ and Ship$^{-/-}$ B cells in response to anti-IgM $F(ab')_2$ stimulation. As expected, ERK2 phosphorylation was reduced in Ship$^{+/-}$ B cells when the BCR

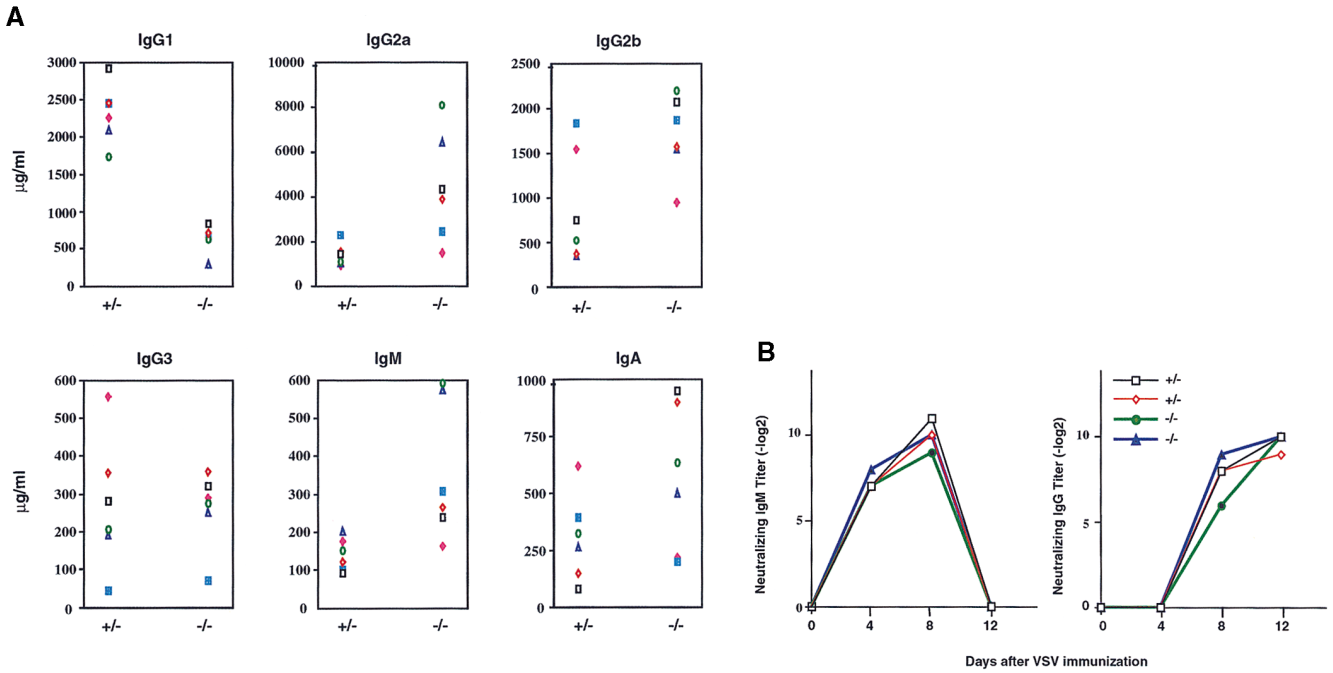

Figure 3. (*A*) Increased basal serum Ig levels in Ship$^{-/-}$Rag-1$^{-/-}$ mice. Unimmunized Ship$^{+/-}$Rag-1$^{-/-}$ and Ship$^{-/-}$Rag-1$^{-/-}$ mice were bled at 8–18 wk of age, and concentrations of serum Ig isotypes were determined by isotype-specific ELISAs. Results from six pairs of experimental mice are shown. (*B*) Normal neutralizing IgM and IgG levels in Ship$^{-/-}$ Rag-1$^{-/-}$ mice after VSV infection. Ship$^{+/-}$Rag-1$^{-/-}$ (+/-) and Ship$^{-/-}$Rag-1$^{-/-}$ (−/−) mice were infected intraperitoneally with VSV, and VSV-neutralizing IgM and IgG titers were determined after infection at the indicated time intervals. Results are representative of six experimental pairs of animals.

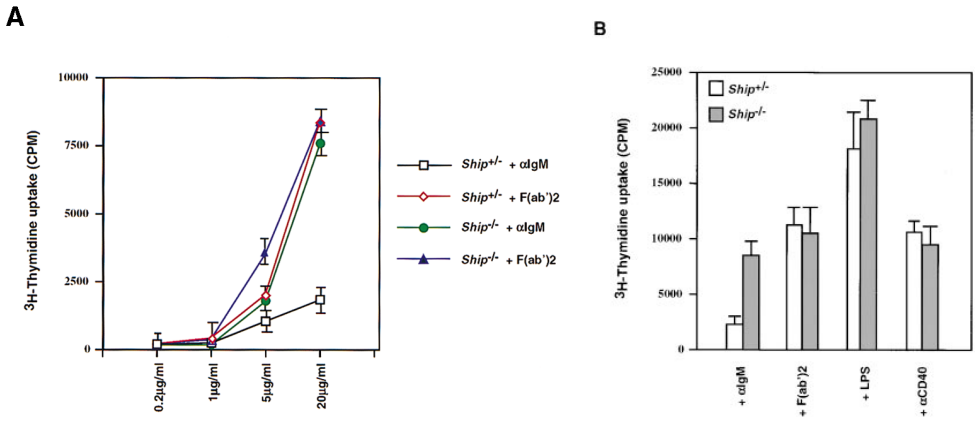

Figure 4. Enhanced proliferative responses of Ship$^{-/-}$ B cells to anti-IgM stimulation. (*A*) Purified splenic B cells were cultured with the indicated amounts of intact goat anti–mouse IgM or of goat anti–mouse IgM F(ab′)$_2$ for 48 h. (*B*) Purified splenic B cells were incubated with 20 μg/ml goat anti–mouse IgM, 15 μg/ml goat anti–mouse IgM F(ab′)$_2$, 2 μg/ml LPS, or 5 μg/ml anti-CD40 for 60 h. Proliferation was assessed by the incorporation of [^{3}H]thymidine. Mean [^{3}H]thymidine uptake ± SD of triplicate cultures of Ship$^{+/-}$ and Ship$^{-/-}$ B cells is shown. Results are representative of three independent experiments.

and FcγRIIB were coligated by intact anti-IgM. In contrast, Ship$^{-/-}$ B cells showed no reduction in ERK2 phosphorylation after intact anti-IgM stimulation, suggesting that Ship plays a role in the downregulation of the MAPK pathway, and that the MAPK pathway is involved in the delivery of the FcγRIIB inhibitory signal.

Discussion

Ship is an inositol phosphatase that plays important roles in signal transduction (5, 20, 23). To investigate Ship's function in lymphocytes, we generated Ship-deficient ES cell lines through homologous recombination, and created Ship$^{-/-}$Rag$^{-/-}$ chimeric mice. Our analyses of Ship$^{-/-}$ Rag$^{-/-}$ chimeras show that Ship is required for immune complex–mediated inhibition of B cell proliferation and the regulation of antibody production. In addition, although the primary function of Ship appears to be one of negative regulation of BCR signaling, our studies suggest that Ship is also involved in pre-B cell maturation and homeostasis of T cell subsets.

The inactivation of Ship in B lymphocytes resulted in enhanced proliferation in response to BCR and FcγRIIB coligation by intact anti-Ig, indicating that FcγRIIB-medi-

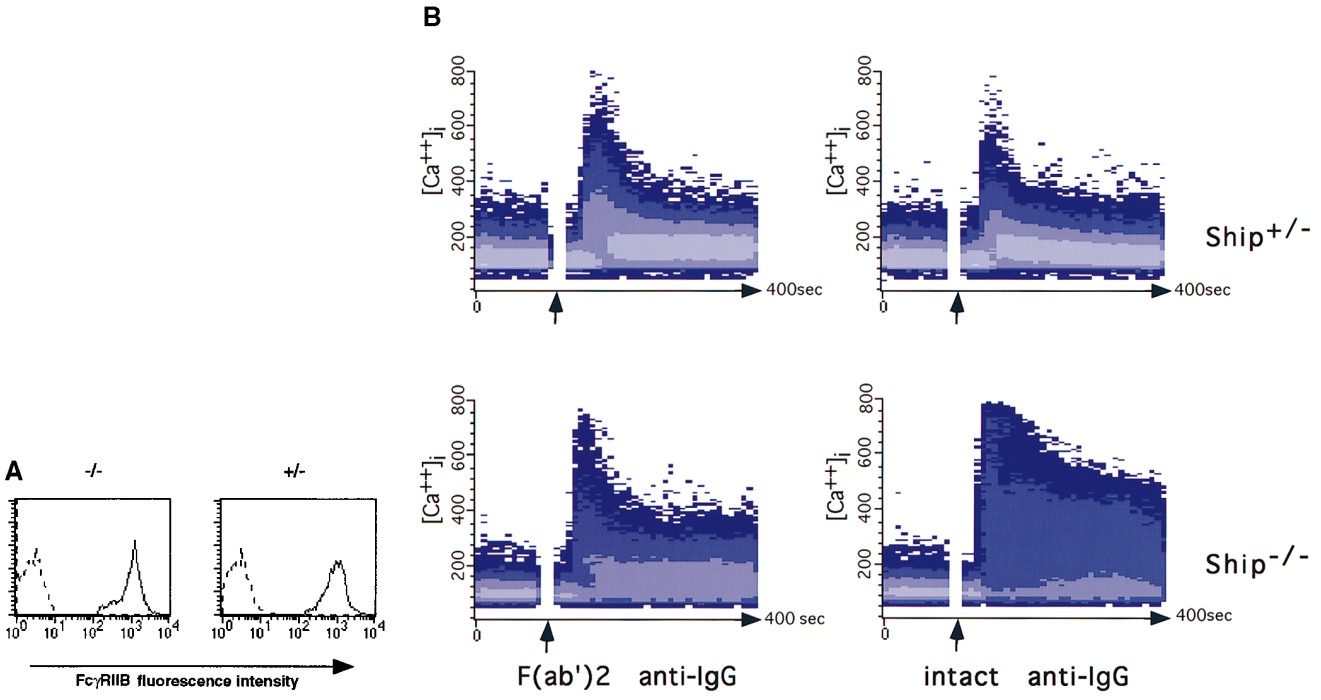

Figure 5. Prolonged Ca^{2+} flux in Ship$^{-/-}$ B cells. (*A*) FcγRIIB expression on B cells. Histogram indicates the expression of FcγRIIB on B cell populations. FcγRIIB was stained with anti-FcγRII/III antibody 2.4G2 (*solid lines*). *Broken line*, Negative staining with anti-Ship antibody. (*B*) Ca^{2+} mobilization. Indo-1–labeled splenocytes were stimulated with 10 μg/ml rabbit anti–mouse IgG or 5 μg/ml rabbit anti–mouse IgG F(ab′)$_2$. *Arrows*, Time point of antibody addition. Results representative of three independent experiments are shown.

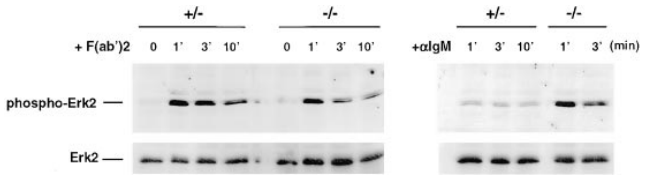

Figure 6. Increased ERK2 phosphorylation in Ship$^{-/-}$ B cells by anti-IgM stimulation. Antiphospho-MAPK immunoblot of whole cell lysates of purified splenic B cells stimulated with 20 μg/ml goat anti–mouse IgM, or 15 μg/ml F(ab′)$_2$ goat anti–mouse IgM, at 37°C for the indicated time period (in minutes). Membranes were stripped and rehybridized to anti-ERK2 antibody to control for loading between lanes. One result representative of three independent experiments is shown.

ated inhibition of BCR signaling is Ship dependent. Ship$^{-/-}$ B cells did not show any defects in other signaling pathways that bypass FcγRIIB, such as stimulation by F(ab′)$_2$, anti-CD40, or LPS; therefore, the predominant role of Ship in resting B cells appears to be confined to the FcγRIIB pathway. We have also noticed that the proliferative responses of Ship$^{-/-}$ B cells to intact anti-Ig were very similar to that of F(ab′)$_2$ stimulation, whereas B cells from *me/me* mice (which are SHP-1–deficient) had a proliferative response to intact anti-Ig stimulation at 40% of their response to F(ab′)$_2$ activation (15). Thus, although SHP-1 may be involved, Ship is the predominant signaling molecule downstream of FcγRIIB.

In B cells, BCR–FcγRIIB coligation triggers molecular events that lead to the inhibition of the Ca^{2+} influx normally initiated by BCR activation, resulting in reduction of BCR signaling (23). In this study, we have shown that the deletion of Ship abrogates FcγRIIB-mediated inhibition of Ca^{2+} influx in B cells. Interestingly, the extent and duration of Ca^{2+} mobilization that occurred in response to BCR–FcγRIIB coligation in the absence of Ship were significantly increased over the Ca^{2+} influx observed in response to BCR activation. Since the prolonged Ca^{2+} mobilization was clearly associated with BCR–FcγRIIB coligation, we speculate that other signaling molecules may be interacting with the phosphorylated ITIM of FcγRIIB in the absence of Ship, and that these interactions generate signals leading to a delayed closing of the membrane Ca^{2+} channels. For example, the phosphorylated ITIM of FcγRIIB has been shown to be an ideal docking site for several SH2-containing proteins, some of which might indirectly modulate Ca^{2+} mobilization (15, 18, 19).

An interesting question is whether modulation of Ca^{2+} mobilization is the sole function of Ship in FcγRIIB signaling. It has been shown that the catalytic domain alone of Ship is capable of delivering the inhibitory effect mediated by FcγRIIB, suggesting direct involvement of the Ship substrates IP4 and/or PIP3 in this signaling process (23). Since IP4 is able to activate the cytoplasmic membrane Ca^{2+} channels (35), it has been postulated that the ITIM of FcγRIIB, once phosphorylated after BCR–FcγRIIB coligation, recruits Ship to the membrane, where it hydrolyzes IP4 and brings the membrane Ca^{2+} channels to a closed state (23, 36). Our results indicate that this is probably not the only function of Ship in delivering FcγRIIB signal, since the MAPK ERK2 was found to be hyperphosphorylated in Ship$^{-/-}$ B cells after BCR–FcγRIIB coligation. We speculate that, once recruited to the membrane and tyrosine phosphorylated, Ship may also modulate the extent of BCR-triggered MAPK signaling through interaction with molecules involved in the BCR pathway. A well-documented interacting partner for Ship is the adapter protein Shc (22, 37). BCR signaling induces the tyrosine phosphorylation of Shc and the subsequent formation of Shc–growth factor receptor–bound protein (Grb)2–Sos complexes, which mediate Ras and MAPK activation (38, 39). However, BCR–FcγRIIB coligation appear to enhance the formation of Ship–Shc complexes and to reduce Shc–Grb2 interaction (37), suggesting that Ship may downregulate the MAPK pathway by competing with Grb2 for Shc binding (40).

Another candidate molecule that may link Ship to BCR signaling is the BCR coreceptor CD19. CD19 becomes rapidly tyrosine phosphorylated after engagement of the BCR (41), but is dephosphorylated upon BCR–FcγRIIB coligation (42, 43). Furthermore, CD19-deficient B cells were unable to respond to FcγRIIB-mediated inhibition (44). Although it is not clear at this point how an inositol phosphatase like Ship could regulate the dephosphorylation of tyrosines in CD19, it is conceivable that Ship is instrumental in the formation of a multiprotein signal transducing complex. It is possible that one component protein of the complex could be a tyrosine phosphatase; for example, Ship has been shown to associate with SHP-2 in hematopoietic cell lines (45).

Although Ship was found to interact with the immunoreceptor tyrosine activation motifs (ITAMs) from the CD3 complex and TCR ζ chain in vitro (46), normal proliferation, IL-2 production, MAPK and SAPK phosphorylation, and Ca^{2+} mobilization were detected in Ship$^{-/-}$ T cells after TCR activation. These findings indicate that Ship is probably not involved in TCR signaling. However, the elevation in the ratio of $CD4^+$ to $CD8^+$ single positive cells in Ship$^{-/-}$ Rag$^{-/-}$ mice, in conjunction with the upregulation of Ship expression in single positive thymocytes after positive selection (47), suggests that Ship plays a role in mature T cells.

The effect of Ship deficiency appeared to be more dramatic in B cells. We observed a significant reduction of the percentage of $B220^+CD25^+sIgM^-$ small pre-B cells in Ship$^{-/-}$Rag$^{-/-}$ chimeric mice. These early B cell populations do not yet express sIgM, suggesting a role of Ship besides inhibition of BCR signaling. The role of Ship in early B cell maturation and the receptor(s) for signaling molecules on which Ship acts during pre-B cell differentiation need to be determined. The percentages of premature IgM^+ and mature IgD^+ B cells were also reduced in bone marrow and peripheral immune organs. This reduction is not caused by a defect in cell proliferation, because Ship$^{-/-}$ B cells showed enhanced proliferative response toward intact antibody stimulation and normal responses toward LPS and anti-CD40 activation (Fig. 4). Since B cells go through negative selection during maturation to assure immunolog-

ical tolerance to self-antigens (48, 49), and since this selection depends on the threshold of intracellular signals (48, 50), deletion of the inhibitory regulator Ship may produce a stronger signal, which exceeds the signaling threshold for negative selection and leads to a greater reduction of bone marrow B cells. Consistent with this hypothesis, we have also observed a shift from $IgM^{hi}IgD^{hi}$ to the more mature $IgM^{lo}IgD^{hi}$ population in $Ship^{-/-}$ B cells, a phenotype normally correlating with B cell hyperresponsiveness caused by the deletion of negative regulators (51).

The enhanced proliferative response of $Ship^{-/-}$ B cells after anti-Ig stimulation and increased basal serum levels of different Ig subclasses suggest a possible deregulation of antibody production in vivo due to the disruption of an immune complex–mediated inhibition. Surprisingly, the Ig levels of neutralizing IgM and IgG after VSV infection were comparable among $Ship^{+/-}Rag^{-/-}$ and $Ship^{-/-}Rag^{-/-}$ chimeric mice, suggesting that additional pathways for maintaining antibody homeostasis are operating in VSV-specific responses. Whether $Ship^{-/-}Rag^{-/-}$ chimeric mice would respond differently to pathogenic stimulation other than VSV remains to be determined.

We thank Kurt Bachmaier, Anne Hakem, Takehiko Sasaki, Yun Kong, and Connie Krawczyk for comments, and Mary Saunders and Marissa Luchico for assistance during preparation of the manuscript. We also give special thanks to Andrew Wakeham, Wilson Khoo, Annick Itie, Arda Shahinian for technical help, and Dr. Tak W. Mak for support.

Address correspondence to Qiurong Liu, Amgen Institute, 620 University Avenue, Suite 706, Toronto, Canada, M5G 2C1. Phone: 416-204-2264; Fax: 416-204-2277; E-mail: qliu@amgen.com

Received for publication 20 April 1998 and in revised form 23 June 1998.

References

1. Damen, E.D., L. Liu, P. Rosten, R.K. Humphries, A.B. Jefferson, P.W. Majerus, and G. Krystal. 1996. The 145-kDa protein induced to associate with Shc by multiple cytokines is an inositol tetraphosphate and phosphatidylinositol 3,4,5-trisphosphate 5-phosphatase. *Proc. Natl. Acad. Sci. USA*. 93:1689–1693.
2. Lioubin, M.N., P.A. Algate, S. Tsai, K. Carlberg, R. Aebersold, and L.R. Rohrschneider. 1996. $p150^{Ship}$, a signal transduction molecule with inositol polyphosphate-5-phosphatase activity. *Genes Dev*. 10:1084–1095.
3. Deuter-Reinhard, M., G. Apell, D. Pot, A. Klippel, L.T. Williams, and W.M. Kavanaugh. 1997. SIP/SHIP inhibits *Xenopus* oocyte maturation induced by insulin and phosphatidylinositol 3-kinase. *Mol. Cell. Biol*. 10:2559–2565.
4. Ono, M., S. Bolland, P. Tempst, and J.V. Ravetch. 1996. Role of the inositol phosphatase SHIP in negative regulation of the immune system by the receptor FcγRIIB. *Nature*. 383: 263–266.
5. Kimura, T., H. Sakamoto, E. Appella, and R.P. Siraganian. 1997. The negative signaling molecule SH2 domain-containing inositol polyphosphate 5-phosphatase (SHIP) binds to the tyrosine-phosphorylated β subunit of the high affinity IgE receptor. *J. Biol. Chem*. 272:13991–13996.
6. Crowley, M.T., S.L. Harmer, and A.L. DeFranco. 1996. Activation-induced association of a 145-kDa tyrosine-phosphorylated protein with Shc and Syk in B lymphocytes and macrophages. *J. Biol. Chem*. 271:1145–1152.
7. Lamkin, T.D., S.F. Walk, L. Liu, J.E. Damen, G. Krystal, and K.S. Ravichandran. 1997. Shc interaction with Src homology 2 domain containing inositol phosphatase (SHIP) *in vivo* requires the Shc-phosphotyrosine binding domain and two specific phosphotyrosines on SHIP. *J. Biol. Chem*. 272:10396–10401.
8. Damen, J.E., L. Liu, R.L. Cutler, and G. Krystal. 1993. Erythropoietin stimulates the tyrosine phosphorylation of Shc and its association with Grb2 and a 145-kd tyrosine phosphorylated protein. *Blood*. 82:2296–2303.
9. Liu, L., J.E. Damen, M.E. Hughes, I. Babic, F.R. Jirik, and G. Krystal. 1997. The Src homology (SH2) domain of SH2-containing inositol phosphatase (SHIP) is essential for tyrosine phosphorylation of SHIP, its association with Shc, and its induction of apoptosis. *J. Biol. Chem*. 272:8983–8988.
10. Köhler, H., B.C. Richardson, D.A. Rowley, and S. Smyk. 1997. Immune response to phosphorylcholine. III. Requirement of the Fc portion and equal effectiveness of IgG subclasses in anti-receptor antibody-induced suppression. *J. Immunol*. 119:1979–1986.
11. Phillips, N.E., and D.C. Parker. 1983. Fc-dependent inhibition of mouse B cell activation of whole anti-μ antibodies. *J. Immunol*. 130:602–606.
12. DeFranco, A.L. 1997. The complexity of signaling pathways activated by the BCR. *Curr. Opin. Immunol*. 9:296–308.
13. Pleiman, C.M., D. D'Ambrosio, and J.C. Cambier. 1994. The B-cell antigen receptor complex: structure and signal transduction. *Immunol. Today*. 15:393–397.
14. Diegel, M.L., B.M. Rankin, J.B. Bolen, P.M. Dubois, and P.A. Kiener. 1994. Cross-linking of Fcγ receptor to surface immunoglobulin on B cells provides an inhibitory signal that closes the plasma membrane calcium channel. *J. Biol. Chem*. 269:11409–11416.
15. Pani, G., M. Kozlowski, J.C. Cambier, G.B. Mills, and K.A. Siminovitch. 1995. Identification of the tyrosine phosphatase PTP1C as a B cell antigen receptor–associated protein involved in the regulation of B cell signaling. *J. Exp. Med*. 181: 2077–2084.
16. Phillips, N.E., and D.C. Parker. 1984. Cross-linking of B lymphocyte Fc-γ receptors and membrane immunoglobulin. *J. Immunol*. 132:627–632.
17. Muta, T., T. Kurosaki, Z. Misulovin, M. Sanchez, M.C. Nussenzweig, and J.V. Ravetch. 1994. A 13-amino-acid motif in the cytoplasmic domain of FcγRIIB modulates B-cell receptor signaling. *Nature*. 368:70–73.

18. Vély, F., S. Olivero, L. Olcese, A. Moretta, J.E. Damen, L. Liu, G. Krystal, J.C. Cambier, M. Daëron, and E. Vivier. 1994. Differential association of phosphatases with hematopoietic co-receptors bearing immunoreceptor tyrosine-based inhibition motifs. *Eur. J. Immunol*. 27:1994–2000.
19. D'Ambrosio, D., K.L. Hippen, S.A. Minskoff, I. Mellman, G.I. Pani, K.A. Siminovitch, and J.C. Cambier. 1995. Recruitment, and activation of PTP1C in negative regulation of antigen receptor signaling by FcγRIIB1. *Science*. 268:293–296.
20. Nadler, M.J.S., B. Chen, J.S. Anderson, H.H. Wortis, and B.G. Neel. 1997. Protein-tyrosine phosphatase SHP-1 is dispensable for FcγRIIB-mediated inhibition of B cell antigen receptor activation. *J. Biol. Chem*. 272:20038–20043.
21. D'Ambrosio, D., D.C. Fong, and J.C. Cambier. 1996. The SHIP phosphatase becomes associated with FcγRIIB1 and is tyrosine phosphorylated during 'negative' signaling. *Immunol. Lett*. 54:77–82.
22. Chacko, G.W., S. Tridandapani, J.E. Damen, L. Liu, G. Krystal, and K.M. Coggeshall. 1996. Negative signaling in B lymphocytes induces tyrosine phosphorylation of the 145-kDa inositol polyphosphate 5-phosphatase, SHIP. *J. Immunol*. 157:2234–2238.
23. Ono, M., H. Okada, S. Bolland, S. Yanagi, T. Kurosaki, and J.V. Ravetch. 1997. Deletion of SHIP or SHP-1 reveals two distinct pathways for inhibitory signaling. *Cell*. 90:293–301.
24. Tybulewicz, V.L.J., C.E. Crawford, P.K. Jackson, R.T. Bronson, and R.C. Mulligan. 1991. Neonatal lethality and lymphopenia in mice with a homozygous disruption of the c-*abl* proto-oncogene. *Cell*. 65:1153–1163.
25. Wurst, W., and A.L. Joyner. 1993. Gene Targeting. Oxford University Press, New York.
26. Wallace, V.A., W.-P. Fung-Leung, E. Timms, D. Gray, K. Kishihara, D.Y. Loh, J. Penninger, and T.W. Mak. 1992. CD45RA and CD45RB^{high} expression induced by thymic selection events. *J. Exp. Med*. 176:1657–1663.
27. Mombaertz, P., J. Iacomini, R.S. Johnson, K. Herrup, S. Tonegawa, and V.E. Papaioannou. 1992. RAG-1-deficient mice have no mature B and T lymphocytes. *Cell*. 68:869–877.
28. Osmond, D.G., A. Rolink, and F. Melchers. 1998. Murine B lymphopoiesis: towards a unified model. *Immunol. Today*. 19: 65–68.
29. Leist, T.P., S.P. Cobbold, H. Waldmann, M. Aguet, and R.M. Zinkernagle. 1987. Functional analysis of T lymphocyte subsets in antiviral host defense. *J. Immunol*. 138:2278–2281.
30. Noelle, R.J., M. Roy, D.M. Shepherd, I. Stamenkovic, J.A. Ledbetter, and A. Aruffo. 1992. A 39-kDa protein on activated helper T cells binds CD40 and transduces the signal of cognate activation of B cells. *Proc. Natl. Acad. Sci. USA*. 89:6550–6554.
31. Heath, A.W., W.W. Wu, and M.C. Howard. 1994. Monoclonal antibodies to murine CD40 define two distinct functional epitopes. *Eur. J. Immunol*. 24:1828–1834.
32. Kashiwada, M., Y. Kaneko, H. Yagita, K. Okumura, and T. Takemori. 1996. Activation of mitogen-activated protein kinases via CD40 is distinct from that stimulated by surface IgM on B cells. *Eur. J. Immunol*. 26:1451–1458.
33. Cyster, J.G., J.I. Healy, K. Kishihara, T.W. Mak, M.L. Thomas, and C.C. Goodnow. 1996. Regulation of B-lymphocyte negative and positive selection by tyrosine phosphatase CD45. *Nature*. 381:325–328.
34. Chan, V.W.F., F. Meng, P. Soriano, A.L. DeFranco, and C.A. Lowell. 1997. Characterization of the B lymphocyte populations in Lyn-deficient mice and the role of Lyn in signal initiation and down-regulation. *Immunity*. 7:69–81.
35. Lückhoff, A., and D. Clapham. 1992. Inositol 1,3,4,5-tetrakisphosphate activates an endothelial Ca^{2+}-permeable channel. *Nature*. 355:356–358.
36. Ravetch, J.V. 1997. Fc receptors. *Curr. Opin. Immunol*. 9:121–125.
37. Tridandapani, S., G.W. Chacko, J.R. Van Brocklyn, and K.M. Coggeshall. 1997. Negative signaling in B cells causes reduced Ras activity by reducing Shc-Grb2 interaction. *J. Immunol*. 158:1125–1132.
38. Saxton, T.M., I. van Oostveen, D. Bowtell, R. Aebersold, and M.R. Gold. 1994. B cell antigen receptor cross-linking induces phosphorylation of the p21^{ras} oncoprotein activators SHC and mSOS1 as well as assembly of complexes containing SHC, GRB-2, mSOS1, and a 145-kDa tyrosine-phosphorylated protein. *J. Immunol*. 153:623–636.
39. Kumar, G., S. Wang, S. Gupta, and A. Nel. 1995. The membrane immunoglobulin receptor utilizes a Shc/Grb2/hSOS complex for activation of the mitogen-activated protein kinase cascade in a B-cell line. *Biochem. J*. 307:215–223.
40. Tridandapani, S., T. Kelley, D. Cooney, M. Pradhan, and K.M. Coggeshall. 1997. Negative signaling in B cells: SHIP Grb2 Shc. *Immunol. Today*. 18:424–427.
41. Tedder, T.F., M. Inaoki, and S. Sato. 1997. The CD19-CD21 complex regulates signal transduction threshold governing humoral immunity and autoimmunity. *Immunity*. 6:107–118.
42. Sato, S., D.A. Steeber, P.J. Jansen, and T.F. Tedder. 1997. CD19 expression levels regulate B lymphocyte development. *J. Immunol*. 158:4662–4669.
43. Kiener, P.A., M.N. Lioubin, L.R. Rohrschneider, J.A. Ledbetter, S.G. Nadler, and M.L. Diegel. 1997. Co-ligation of the antigen and Fc receptors gives rise to the selective modulation of intracellular signaling in B cells. *J. Biol. Chem*. 272:3838–3844.
44. Hippen, K.L., A.M. Buhl, D. D'Ambrosio, K. Nakamura, C. Persin, and J.C. Cambier. 1997. FcγRIIB1 inhibition-mediated phosphoinositide hydrolysis and Ca^{2+} mobilization is integrated by CD19 dephosphorylation. *Immunity*. 7:49–58.
45. Sattler, M., R. Salgia, G. Shrikhande, S. Verman, J.-L. Choi, L.R. Rohrschneider, and J.D. Griffin. 1997. The phosphatidylinositol polyphosphate 5-phosphatase SHIP and the protein tyrosine phosphatase SHP-2 form a complex in hematopoietic cells which can be regulated by BCR/ABL and growth factors. *Oncogene*. 15:2370–2384.
46. Osborne, A., G. Zenner, M. Lubinus, X. Zhang, Z. Songyang, L.C. Cantley, P. Majerus, P. Burn, and J.P. Kochan. 1996. The inositol 5′-phosphatase SHIP binds to immunoreceptor signaling motifs and responds to high affinity IgE receptor aggregation. *J. Biol. Chem*. 217:29271–29278.
47. Liu, Q., F. Shalaby, J. Jones, D. Bouchard, and D.J. Dumont. 1998. The SH2-containing inositol polyphosphate 5-phosphatase, Ship, is expressed during haematopoiesis and spermatogenesis. *Blood*. 91:1–8.
48. Goodnow, C.C. 1996. Balancing immunity and tolerance: deleting and tuning lymphocyte repertoires. *Proc. Natl. Acad. Sci. USA*. 93:2264–2271.
49. Hartley, S.B., M.P. Cooke, D.A. Fulcher, A.W. Harris, S. Cory, A. Basten, and C.C. Goodnow. 1993. Elimination of self-reactive B lymphocytes proceeds in two stages: arrested development and cell death. *Cell*. 72:325–335.
50. Klinman, N.R. 1996. The "clonal selection hypothesis" and current concepts of B cell tolerance. *Immunity*. 5:189–195.
51. O'Keefe, T.L., G.T. Williams, S.L. Davies, and M.S. Neuberger. 1996. Hyperresponsive B cells in CD22-deficient mice. *Science*. 274:798–801.